

PDF hosted at the Radboud Repository of the Radboud University Nijmegen

The following full text is a preprint version which may differ from the publisher's version.

For additional information about this publication click this link.

<http://hdl.handle.net/2066/75201>

Please be advised that this information was generated on 2017-12-06 and may be subject to change.

Majority-spin non-quasiparticle states in half-metallic ferrimagnet Mn_2VAl

L. Chioncel,^{1,2} E. Arrigoni,¹ M.I. Katsnelson,³ and A.I. Lichtenstein⁴

¹*Institute of Theoretical Physics, Graz University of Technology, A-8010 Graz, Austria*

²*Faculty of Science, University of Oradea, RO-410087 Oradea, Romania*

³*Institute for Molecules and Materials, Radboud University of Nijmegen, NL-6525 ED Nijmegen, The Netherlands*

⁴*Institute of Theoretical Physics, University of Hamburg, DE-20355 Hamburg, Germany*

The density of non-quasiparticle states in the ferrimagnetic full-Heuslers Mn_2VAl alloy is calculated from first principles upon appropriate inclusion of correlations. In contrast to most half-metallic compounds, this material displays an energy gap in the majority-spin spectrum. For this situation, non-quasiparticle states are located below the Fermi level, and should be detectable by spin-polarized photoemission. This opens a new way to study many-body effects in spintronic-related materials.

Half metals display a particular type of itinerant-electron magnetism as well as unusual electronic properties: they are metallic for one spin channel, and insulating or semiconducting for the opposite one [1, 2]. Electronic structure calculations based on density functional theory offer an explanation for the half-metallicity based on the interplay between the crystal structure, the valence electron count, the covalent bonding, and the large exchange splitting in addition to symmetry constraints. The expected 100% spin polarization of half-metals turned out to be an excellent motivation in developing the field of spintronics both from a theoretical and an experimental point of view [2, 3]. In reality many potential half-metallic ferromagnets exhibit a dramatic decrease of bulk spin polarization at temperatures well below their Curie temperature. In order to understand such a behavior from a theoretical point of view it is necessary to consider finite temperature many-body effects [2].

An important effect of dynamical electron correlations in half-metals is the existence of non-quasiparticle (NQP) states [4, 5, 6]. These states contribute significantly in reducing the tunneling transport in heterostructures containing HMF [7, 8, 9, 10, 11], even in the presence of disorder. NQP states strongly influence the value and temperature dependence of the spin polarization in HMF [2, 6, 12], which is of primary interest for potential applications. These states originate from spin-polaron processes whereby the minority spin low-energy electron excitations, which are forbidden for HMF in the single-particle picture, are possible as superpositions of majority-spin electron excitations and virtual magnons [2, 4, 5, 6]. Recently we have applied the LDA+DMFT (local density approximation plus dynamical mean field theory) method (for review of this approach, see Ref.13) to describe from first principles the non-quasiparticle states in several half-metals [14, 15, 16, 17, 18]. Up to now, our studies were restricted to half metals with a gap in the *minority* spin channel. In this situation NQP states appear just *above* the Fermi level [6].

On the contrary, it was predicted that in half-metallic materials with a gap in the majority (say, “up”) spin

channel, NQP states should appear below the Fermi level [4, 5, 6]. This asymmetry can be understood in terms of electron-magnon scattering processes, as presented in the followings.

A well studied model which takes into account the interaction of charge carriers with local moments is the *s-d* exchange model. The interacting part of the Hamiltonian is given by $-I \sum \mathbf{S}_i \sigma_{\alpha\beta} c_{i\alpha}^\dagger c_{i\beta}$, where I is the *s-d* exchange parameter, \mathbf{S}_i represents the localized spin operators, $\sigma_{\alpha\beta}$ are the Pauli matrices, and $c_{i\sigma}$ are operators for conduction electrons. The NQP picture turns out to be essentially different for the two possible signs of the *s-d* exchange parameter.

The ground state of the system with $I > 0$ (assuming that the Fermi energy is smaller than the spin splitting $2IS$) has maximum spin projection and, thus, the minority-electron band should be empty. For this case ($I > 0$), NQP states in the minority spin gap develop as a superposition of the majority-electron states plus magnon states, and of the minority-electron states, so that the *total* spin projection of the system is conserved. As a result of this spin-polaronic effect, the minority-electron density of states has a tail corresponding to the virtual conduction electron spin-flip processes with magnon emission. However, these virtual flips are impossible below the Fermi energy E_F due to the Pauli principle (all majority-electron states are already occupied and thus unavailable). Therefore, for the positive *s-d* exchange interaction the NQP states form above E_F .

Contrary, for negative I the minority-spin band lies below the majority-spin one [2, 6]. Occupied minority-spin states can be superposed with majority-electron states plus magnons, with conserved total spin projection, so the NQP states occur below E_F . At the same time, for $I < 0$ the ferromagnetic ground state is non-saturated and thus zero-point magnon fluctuations are allowed. It is the fluctuations which are responsible for formation of *occupied* majority-electron NQP states there.

Formally, the difference between $I < 0$ and the previous $I > 0$ cases, can be explained in terms of a particle-hole transformation $c_{i\sigma}^\dagger \rightarrow d_{i\bar{\sigma}}$, and $c_{i\sigma} \rightarrow d_{i\bar{\sigma}}^\dagger$. This modifies the *s-d* exchange Hamiltonian into $I \sum \mathbf{S}_i \sigma_{\alpha\beta} d_{i\alpha}^\dagger d_{i\beta}$.

In other words, the Hamiltonian with $I > 0$ for electrons is equivalent to that with $I < 0$ for holes.

The above argument based on the s - d exchange model can be generalized for arbitrary multi-band half-metallic electronic structures [2, 6]. The conclusion remain unchanged: *for the case of minority-electron gap, NQP states are situated above the Fermi energy, while for the cases when the gap is present for majority-electrons, NQP states are formed below the Fermi energy.*

Most HMF materials have a gap in the minority spin channel so that NQP states arise above the Fermi level. As a consequence, these states cannot be studied by the very well-developed and accurate technique of spin-polarized photoemission [19], which can only probe occupied states. The spin-polarized Bremsstrahlung Isochromat Spectroscopy (BIS) probing unoccupied states [20] has a much lower resolution. For this reason, HMF with a gap in the majority-spin channel, and, consequently, NQP states in the occupied region of the spectrum, allow for a detailed experimental analysis of these correlation-induced states and are, therefore, potentially of great interest. It is the purpose of the present work to perform an electronic structure calculation based on a combination of the generalized-gradient approximation (GGA) and of DMFT for the half-metallic ferrimagnetic full-Heusler alloy Mn_2VAl , which has a gap in the majority spin channel. By appropriately taking into account effects due to electronic correlations, we demonstrate explicitly the existence of majority spin NQP states arising just below the Fermi level, and study the temperature dependence of their spectral weight.

In full Heusler compounds with the formula X_2YZ , Mn atoms usually occupy the Y-position, while compounds in which Mn assumes the X-position Mn_2YZ , are very rare. The prototype from the latter category is Mn_2VAl , for which a large number of theoretical and experimental investigations have been made. Neutron diffraction experiments [21] demonstrated the existence of a ferrimagnetic state in which Mn has a magnetic moment of $1.5 \pm 0.3 \mu_B$ and V moment is $-0.9 \mu_B$. X-ray diffraction and magnetization measurements [22] found a total magnetic moment of $1.94 \mu_B$ at $5K$, close to the half-metallic value of $2 \mu_B$. The Curie temperature of the sample was found to be about $760K$ and the loss of half-metallic character was attributed to the small amount of disorder. Electronic-structure calculations performed by Ishida [23] within the local-density approximation (LDA), predict the ground state of Mn_2VAl to be close to half-metallicity. Weht and Pickett [24] used the GGA for the exchange correlation potential and showed that Mn_2VAl is a half-metallic ferrimagnet with atomic moments in very good agreement with the experiment. Recent calculations of the exchange parameters for Mn_2VAl [25] show a strong $Mn-V$ exchange interaction that influence the ordering in the Mn sublattice. The estimated Curie temperatures are in good agreement with the experimental values [25].

The intermixing between V and Al atoms in the Mn_2VAl alloy showed that a small degree of disorder decreases the spin polarization at the Fermi level from its ideal 100% value, but the resulting alloy $\text{Mn}_2\text{V}_{1-x}\text{Al}_{1+x}$ still show an almost half-metallic behavior [26, 27].

According to the ideal full Heusler ($L2_1$) structure, the V atom occupy the $(0, 0, 0)$ position, the Mn atoms are situated at $(1/4, 1/4, 1/4)a$ and $(3/4, 3/4, 3/4)a$, and the Al at $(1/2, 1/2, 1/2)a$, where $a = 5.875\text{\AA}$ is the lattice constant of the Mn_2VAl compound. In our work, correlation effects in the valence V and Mn d orbitals are included via an on-site electron-electron interaction in the form $\frac{1}{2} \sum_{i\{m,\sigma\}} U_{mm'm''m'''} c_{im\sigma}^\dagger c_{im'\sigma'}^\dagger c_{im''\sigma''} c_{im'''\sigma'''} c_{im''\sigma''}$. The interaction is treated in the framework of dynamical mean field theory (DMFT) [13], with a spin-polarized T-matrix Fluctuation Exchange (SPTF) type of impurity solver [28]. Here, $c_{im\sigma}/c_{im\sigma}^\dagger$ destroys/creates an electron with spin σ on orbital m on lattice site i . The Coulomb matrix elements $U_{mm'm''m'''}$ are expressed in the usual way [29] in terms of three Kanamori parameters U , $U' = U - 2J$ and J . Typical values for Coulomb ($U = 2\text{eV}$) and Stoner ($J = 0.93\text{eV}$) parameters were used for Mn and V atoms. The above value of U is considerably smaller than the bandwidth of Mn_2VAl ($7-8\text{eV}$) therefore the use of a perturbative SPTF-solver is justified. In addition, the same solver was used to investigate spectroscopic properties of transition metals with remarkable results [30, 31, 32, 33, 34].

Since the static contribution from correlations is already included in the local spin-density approximation (LSDA/GGA), so-called “double counted” terms must be subtracted. To achieve this, we replace $\Sigma_\sigma(E)$ with $\Sigma_\sigma(E) - \Sigma_\sigma(0)$ [35] in all equations of the DMFT procedure [13]. Physically, this is related to the fact that DMFT only adds *dynamical* correlations to the LSDA/GGA result. For this reason, it is believed that this kind of double-counting subtraction “ $\Sigma(0)$ ” is more appropriate for a DMFT treatment of metals than the alternative static “Hartree-Fock” (HF) subtraction [36].

In Fig. 1 we present the total density of states computed in GGA and GGA+DMFT, for $T=200K$. The GGA density of states displays a gap of about 0.4eV in the majority spin channel in agreement with previous calculations [24]. As expected from the s - d model calculation, majority spin NQP states are visible just below the Fermi level, with a peak around -0.25eV . In order to evaluate the spectral weight of these NQP states, we fit the low-energy density of states below the Fermi level in the majority channel with a Gaussian centered around the peak position. The NQP spectral weight is then defined as the area below the Gaussian curve. The inset shows the NQP spectral weight for several temperatures up to $300K$. It is interesting to note that within the computed temperature range $50 \leq T \leq 300$ these values are almost constant and considerably larger in comparison with similar values for $(\text{NiFe})\text{MnSb}$ [16]. The data pre-

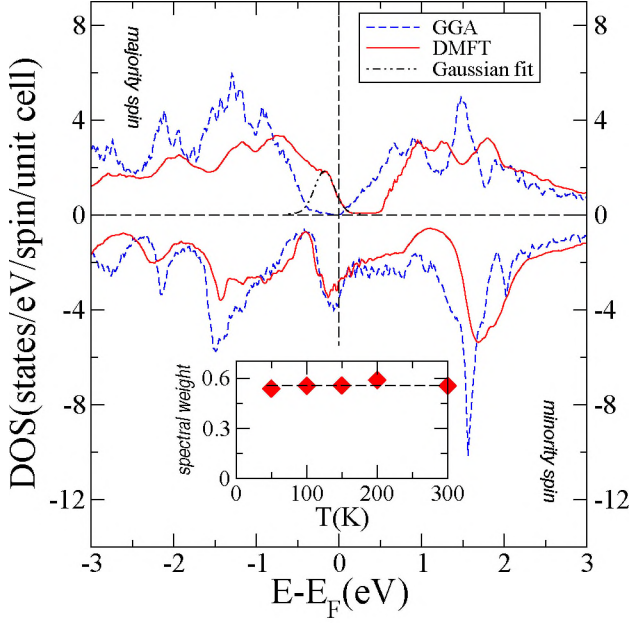


FIG. 1: (color online) Total density of states, computed within GGA (dashed/blue), and GGA+DMFT (full/red). The Gaussian fit to the density of NQP states is shown as a dotted-dashed (black) line just below the Fermi level for the majority spin channel. The temperature dependent spectral weight of NQP states is displayed in the inset.

sented in the inset can be extrapolated down to $T = 0K$, and a spectral weight of $\approx 0.544 \pm 0.018$ (states/Mn-d) is obtained. This demonstrates that NQP states are present also at $T=0K$, and obviously they are not captured by the mean-field, GGA result. As it will be discussed below, NQP states predominantly consist of $Mn-d$ electrons, so the value for the integrated spectral weight (inset of Fig. 1) only comes from $Mn-d$ orbitals.

The atom resolved DOS is presented in Fig. 2. In GGA, the net magnetic moment per unit cell is $2\mu_B$ with parallel Mn moments having values close to $1.6\mu_B$ and oppositely oriented V moments close to $-0.8\mu_B$. Below the gap, the majority spin total DOS is mainly of Mn character. The Mn and V moments have a strong t_{2g} character, and a small Al contribution to the magnetic moment is present. Most of the V majority spin states lie above the gap, along with the Mn e_g states. Minority-spin states below $0.5eV$ have roughly an equal amounts of V(t_{2g}) and Mn character. States around the Fermi energy have a predominant $Mn(t_{2g})$ character, in agreement with [24]. In contrast to the GGA results, the many-body DMFT calculation (see Fig. 2) yields a significant DOS for the majority spin states just below the Fermi level. These are the *majority spin NQP states* discussed above [12, 14, 15, 16, 17, 18]. As can be seen in Fig. 2 majority spin NQP states are predominantly of $Mn - 3d^1$ character. Their spectral weight is quite

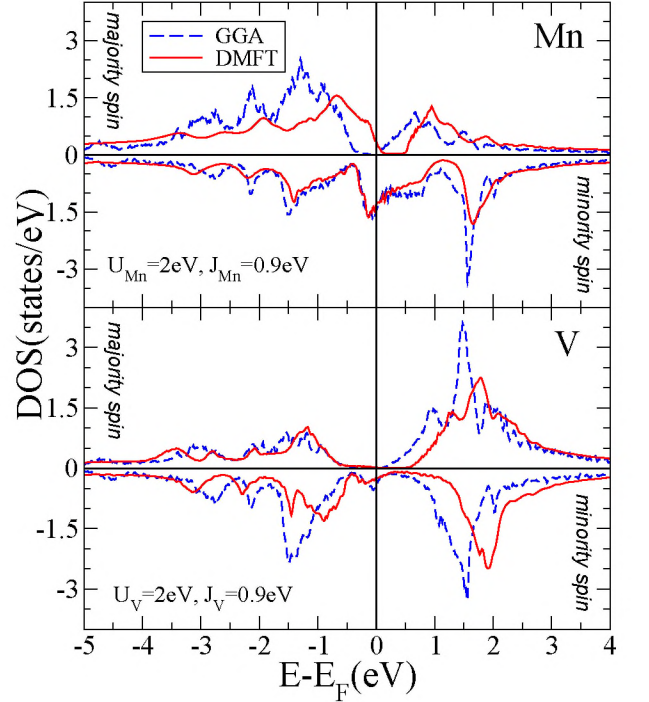


FIG. 2: (color online) Atom resolved density of states, computed within the GGA (dashed/blue) and GGA+DMFT (full/red) approach, at $T=200K$. The majority spin NQP states are visible in the Mn- $3d^1$ DOS just below the Fermi level.

significant (see inset of Fig. 1) so that accurate spin-polarized photoemission experiments should be able to identify the existence of such states. In contrast, majority spin V(t_{2g}) states below the Fermi energy are not significantly changed. Above the Fermi level, the Mn(e_g) and V(e_g) states are pushed to higher energy, such that a gap is formed just above E_F . In the minority spin channel below E_F , both V and Mn(t_{2g}) states are slightly modified, while above E_F , V(e_g) states are shifted to higher energies by $0.5eV$. Around the Fermi level, the dominant $Mn - 3d^1$ DOS is not significantly changed with respect to the GGA values.

The applicability of the local DMFT approach to the problem of the existence of NQP states has been discussed in ref. [2] and [14]. It is essential to stress that the accurate description of the magnon spectrum is not important for the existence of nonquasiparticle states and for the proper estimation of their spectral weight, but can be important to describe an explicit shape of the density of states “tail” in a very close vicinity of the Fermi energy.

The imaginary part of the atom and orbital resolved self-energies, for $T=200K$ are presented in Fig. 3. For the minority Mn- e_g , V- e_g and V- t_{2g} -orbitals we observe that the imaginary part of the self-energy has a rather symmetric energy dependence around the Fermi level, with a normal Fermi-liquid-type behavior $-Im\Sigma_{Mn/V}^{\downarrow}(E) \propto$

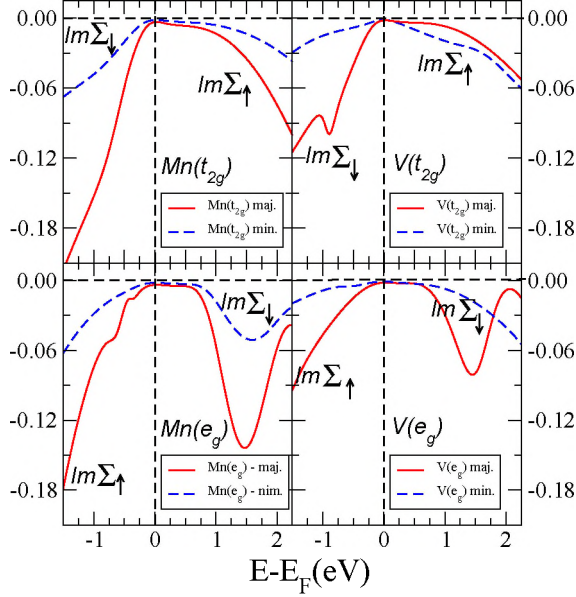


FIG. 3: (color online) Imaginary part of the self-energies $Im\Sigma_{Mn/V}^\sigma$ for t_{2g} -orbitals on Mn (left upper panel) and V (right upper panel). The solid (red) line shows results for the majority(\uparrow) spins, while the dashed (blue) line for minority spins. The lower panels show the corresponding $Im\Sigma_{Mn/V}^\sigma$ for the e_g orbitals.

$(E - E_F)^2$. The majority spin $-Im\Sigma_{Mn/V}^\uparrow(E)$ shows a significant increase right below the Fermi level which is more pronounced for the t_{2g} -orbitals. In addition, a slight kink is evidenced for an energy around -0.25eV . The majority-state nonquasiparticles are visible in the majority spin channel Fig. 2 at about the same energy. These results shown in Fig. 3 suggests that many-body effects are stronger on Mn than on V sites. Therefore, NQP states are mainly determined by the $Mn-d$ atoms.

The behavior of the imaginary part of the self-energy (Fig. 3) and the Green function (Fig. 2) can be correlated with the analysis of the spin-resolved optical conductivity. We have estimated the latter for different temperatures within the GGA and GGA+DMFT approaches using an approximation of constant matrix elements. Already at 50K the majority-spin optical spectra shows the appearance of a Drude peak signaling the closure of the majority spin gap. With increasing temperatures, spectral weight is transferred towards the Drude peak contributing to the depolarization discussed below in Fig. 4.

As it was demonstrated previously [2, 4, 5, 6], the non-quasiparticle spectral weight in the density of states (Fig. 2) is proportional to the imaginary part of the self-energy (Fig. 3), therefore it is determined by the quasiparticle decay, which is the reason for the name of these states.

Fig. 4 displays the temperature dependence of the

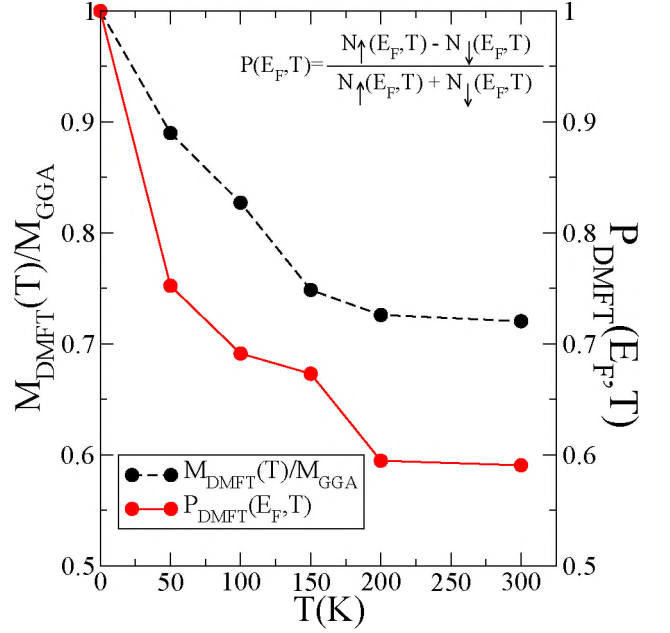


FIG. 4: (color online) Temperature dependence of the spin polarization of conduction electrons (full/red) at the Fermi level $P(E_F, T)$, and normalized magnetization $M(T)/M(0)$ (dashed/black).

magnetization obtained directly from the GGA+DMFT calculations and the spin polarization at the Fermi level, obtained using the relation $P(E_F, T) = (N_\uparrow(E_F, T) - N_\downarrow(E_F, T)) / (N_\uparrow(E_F, T) + N_\downarrow(E_F, T))$, N_σ being the density of states. These results reflect a general trend valid for half-metals in the presence of NQP states [2, 11, 14, 15, 16, 17, 18], namely that magnetization and polarization behave differently as function of temperature. However, as can be seen in Fig. 4, this difference is not as sharp as in other HMF materials [12, 18].

The effect of disorder on half-metallicity was recently discussed in $Mn_2V_{1-x}Al_{1+x}$ alloys, for $-0.2 \leq x \leq 0.2$ [22, 26, 27]. The excess of both Al and V atoms ($x = 0.1 / -0.1$ or $x = 0.2 / -0.2$) has the effect of shrinking the gap to zero, but with the Fermi level situated within the gap. In addition, the Mn moment is not affected by disorder and remains constant, in contrast to the V moment. Spin polarization is decreased by about 10%, with electrons around the Fermi level having a dominant minority spin character [26]. In contrast, many-body correlations have a much more dramatic effect. For non-zero temperatures, all atomic magnetizations are decreased. For instance, near room temperature ($T = 300\text{K}$) the strongest decrease occurs in V, for which the moment drops almost by 47%, the Mn moment is reduced by 32%, while the Al experiences just a small reduction by 4%. As one can see from Fig. 4, already at 50K polarization drops to 75%, and is further decreased upon increasing the temperature. As we discussed previously for

the case of FeMnSb [16], many-body induced depolarization is significantly stronger than the effect of disorder or of other spin-mixing mechanisms such as spin-orbit coupling. This observation seems to hold also for the case of Mn_2VAl , although we can not exclude the fact that for a larger degree of disorder, the material could possibly depart from its almost half-metallic situation displayed for small degree of substitution ($-0.2 < x < 0.2$).

In conclusion, in this paper we have shown for a specific material that NQP states are also present in half-metals with a gap in the majority spin channel, and appear just below the Fermi level, as predicted in model calculations [5]. In the case of Mn_2VAl , these states mainly consist of $Mn-3d^\uparrow$ electrons and have a considerable spectral weight. Although this material was reported to be a half-metal from electronic structure calculations [24], the experimental evidence is not clear. Several reasons are invoked such as existence of defects or the reduced symmetry at surface and interfaces. From a theoretical point of view, we show that correlation-induced NQP states significantly change the majority spin electronic states, thus reducing the spin polarization at E_F . The appearance of NQP states and its connection with tunneling magnetoresistance was recently studied in Co_2MnSi -based tunnel magnetic junction [12]. A great challenge would be to produce TMR junctions based on the ferri-magnetic Mn_2VAl . This would allow for a direct experimental investigation of the existence of majority spin NQP states. Promising candidate HMF materials with a majority spin gap of similar magnitude as Mn_2VAl are the double perovskites Sr_2FeMO_6 ($M=\text{Mo,Re}$) or $\text{Sr}_2\text{CrReO}_6$ often associated with colossal magnetoresistance behavior. In particular the electronic structure of $\text{Sr}_2\text{CrReO}_6$ shows a closure of its majority spin gap in the presence of spin-orbit coupling [37], with states having a small spectral weight symmetrically distributed around the Fermi energy. Discrepancies between the experiment and theoretical computations were explained based on possible anti-site disorder [37]. We suggest that a significant density of NQP states could be present in the above perovskites as well. Work on these lines is in progress.

L.C. and E.A. acknowledge financial support by the Austrian science fund under project nr. FWF P18505-N16. L.C. also acknowledge the financial support offered by Romanian Grant CNCIS/ID672/2009. M.I.K. acknowledges financial support from FOM (The Netherlands). A.I.L. acknowledge financial support from the DFG (Grants No. SFB 668-A3).

[1] R. A. de Groot, F. M. Mueller, P. G. van Engen, and K. H. J. Buschow, Phys. Rev. Lett. **50**, 2024 (1983).
 [2] M. I. Katsnelson, V. Y. Irkhin, L. Chioncel, A. I. Lichtenstein, and R. A. de Groot, Reviews of Modern Physics **80**, 315 (2008).

[3] I. Zutic, J. Fabian, and S. D. Sarma, Rev. Mod. Phys. **76**, 323 (2004).
 [4] D. M. Edwards and J. A. Hertz, Journal of Physics F-Metal Physics **3**, 2191 (1973).
 [5] V. Y. Irkhin and M. I. Katsnelson, J. Phys.: Condens. Matter **2**, 7151 (1990).
 [6] V. Y. Irkhin and M. I. Katsnelson, Phys. Usp. **37**, 659 (1994).
 [7] V. Y. Irkhin and M. I. Katsnelson, Eur. Phys. J. B **30**, 481 (2002).
 [8] E. McCann and V. I. Fal'ko, Phys. Rev. B **68**, 172404 (2003).
 [9] G. Tkachov, E. McCann, and V. I. Fal'ko, Phys. Rev. B **65**, 024519 (2001).
 [10] E. McCann and V. I. Fal'ko, Phys. Rev. B **66**, 134424 (2002).
 [11] V. Y. Irkhin and M. I. Katsnelson, Phys. Rev. B **73**, 104429 (2006).
 [12] L. Chioncel, Y. Sakuraba, E. Arrigoni, M. I. Katsnelson, M. Oogane, Y. Ando, T. Miyazaki, E. Burzo, and A. I. Lichtenstein, Phys. Rev. Lett. **100**, 086402 (2008).
 [13] G. Kotliar, S. Y. Savrasov, K. Haule, V. S. Oudovenko, O. Parcollet, and C. A. Marianetti, Rev. Mod. Phys. **78**, 865 (2006).
 [14] L. Chioncel, M. I. Katsnelson, R. A. de Groot, and A. I. Lichtenstein, Phys. Rev. B **68**, 144425 (2003).
 [15] L. Chioncel, M. I. Katsnelson, G. A. de Wijs, R. A. de Groot, and A. I. Lichtenstein, Phys. Rev. B **71**, 085111 (2005).
 [16] L. Chioncel, E. Arrigoni, M. I. Katsnelson, and A. I. Lichtenstein, Phys. Rev. Lett. **96**, 137203 (2006).
 [17] L. Chioncel, P. Mavropoulos, M. Ležaić, S. Blügel, E. Arrigoni, M. I. Katsnelson, and A. I. Lichtenstein, Phys. Rev. Lett. **96**, 197203 (2006).
 [18] L. Chioncel, H. Allmaier, A. Yamasaki, M. Daghofer, E. Arrigoni, M. Katsnelson, and A. Lichtenstein, Phys. Rev. B **75**, 140406 (2007).
 [19] P. D. Johnson, Rep. Prog. Phys. **60**, 1217 (1997).
 [20] M. Donath, Surf. Sci. Rep. **20**, 251 (1994).
 [21] H. Itoh, T. Nakamichi, Y. Yamagichi, and N. Kazama, Trans. Japan. Inst. Met. **24**, 256 (1983).
 [22] C. Jiang, M. Venkatesan, and J. M. D. Coey, Solid State Commun. **118**, 513 (2001).
 [23] S. Ishida, S. Asano, and J. Ishida, J. Phys. Soc. Jpn. **53**, 2718 (1984).
 [24] R. Weht and W. E. Pickett, Phys. Rev. B **60**, 13006 (1999).
 [25] E. Sasioglu, L. M. Sandratskii, and P. Bruno, J. Phys.: Condens. Matter **17**, 995 (2005).
 [26] K. Ozdogan, I. Galanakis, E. Sasioglu, and B. Aktas, J. Phys.: Condens. Matter **18**, 2905 (2006).
 [27] I. Galanakis, K. Özdoğan, E. Şasioglu, and B. Aktas, Phys. Rev. B **75**, 092407 (2007).
 [28] M. I. Katsnelson and A. I. Lichtenstein, Eur. Phys. J. B **30**, 9 (2002).
 [29] M. Imada, A. Fujimori, and Y. Tokura, Rev. Mod. Phys. **70**, 1039 (1998).
 [30] J. Minár, L. Chioncel, A. Perlov, H. Ebert, M. I. Katsnelson, and A. I. Lichtenstein, Phys. Rev. B **72**, 045125 (2005).
 [31] J. Minar, H. Ebert, C. D. Nadai, N. B. Brookes, F. Venturini, G. Ghiringhelli, L. Chioncel, M. I. Katsnelson, and A. I. Lichtenstein, Phys. Rev. Lett. **95**, 166401 (2005).

- [32] J. Braun, J. Minár, H. Ebert, M. I. Katsnelson, and A. I. Lichtenstein, Phys. Rev. Lett. **97**, 227601 (2006).
- [33] S. Chadov, J. Minár, H. Ebert, A. Perlov, L. Chioncel, M. I. Katsnelson, and A. I. Lichtenstein, Phys. Rev. B **74**, 140411 (2006).
- [34] A. Grechnev, I. Di Marco, M. I. Katsnelson, A. I. Lichtenstein, J. Wills, and O. Eriksson, Phys. Rev. B **76**, 035107 (2007).
- [35] A. I. Lichtenstein, M. I. Katsnelson, and G. Kotliar, Phys. Rev. Lett. **87**, 067205 (2001).
- [36] A. G. Petukhov, I. I. Mazin, L. Chioncel, and A. I. Lichtenstein, Phys. Rev. B **67**, 153106 (2003).
- [37] G. Vaitheeswaran, V. Kanchana, and A. Delin, Appl. Phys. Lett. **86**, 032513 (2005).